DOI: https://doi.org/10.62985/j.huit_ojs.vol24.no4.99

CONTROL OF UNIFIED POWER QUALITY CONDITIONER UNDER GRID VOLTAGE SAG AND NONLINEAR LOADS

Nguyen Thi Thanh Truc, Van Tan Luong*, Huynh Nhat Quang

Ho Chi Minh City University of Industry and Trade

*Email: *luongvt@huit.edu.vn*

Received: 9 January 2024; Accepted: 8 March 2024

ABSTRACT

In this paper, a control scheme based on feedback linearization (FL) control technique with or without resonant control for unified power quality conditioner (UPQC) which is known as series active filter and shunt active filter, is proposed to compensate both the load voltages and grid currents under grid voltage sags and nonlinear loads. A nonlinear model of the system consisting of series active filter and shunt active filter in the dq synchronous reference frames is derived. The load voltage based on FL with resonant control and grid current controllers based on only FL in dq components is designed, depending on series and shunt active filters, respectively. With the proposed scheme, the load voltages are regulated to reach the rated value and both waveforms of load voltages and grid currents are controlled to become almost sinusoidal, compared with the proportional-integral (PI) controller. Simulation results are given to prove the effectiveness of the proposed method.

Keywords: Unified power quality conditioner (UPQC), nonlinear loads, nonlinear theory, voltage sags.

1. INTRODUCTION

Voltage sags/drops are considered as one of the most common and costly power quality issues which affect sensitive loads. They can cause interruptions for electronic equipment and large losses in industrial processes [1, 2]. The series active power filter (APF), known as the dynamic voltage restorer (DVR), is one of the most effective solutions for protecting sensitive loads from voltage sags [3-6]. The DVR is connected in series through series transformers between the grid-side and load-side so that the load voltages are maintained to be balanced and sinusoidal at the desired value during the grid voltage sag occurrence. Passive filters [7], shunt active power filters (APFs) [8, 9], and hybrid APFs [10] are used to suppress the grid current harmonics. However, most of them can only solve one or two power quality issues.

Recently, unified power quality conditioners (UPQCs) have been introduced and considered as an effective solution to handle problems related to various currents and voltages. An UPQC, consisting of shunt and series APFs, can compensate for the load voltage distortions as well as grid current harmonics so that the load voltages and the grid currents are controlled to become purely sinusoidal. As for the control scheme, a cascaded proportional-integral (PI) controller consisting of outer voltage control and inner current control loops for the d-q components has been applied [5, 11]. However, the control dynamic response using PI is not so fast due to the limitation of bandwidth of the voltage control loop [5]. In addition, the components of negative sequence and zero-sequence occur in the grid voltage during unbalanced sags conditions. On the other hand, the grid voltage which is transformed into the

rotating reference frame can be alternating current (AC) signals under grid unbalanced sags. Meanwhile, a conventional PI controller is used for regulating only direct current (DC) signals. To overcome this issue, a proportional resonant (PR) or proportional integral plus resonant (PIR) control has been employed to control the UPQC, so that the load voltages are much compensated to become sinusoidal and reach rated value in the cases of both unbalanced grid voltage drop and nonlinear loads [12]. However, the performance of both PI and PR/PIR linear control methods with a nonlinear model will be significantly deteriorated. Another method is that the nonlinear control of the UPS or DVR is considered [13, 14]. Therefore, the nonlinear control gives better performance than the control schemes depending on the PI control.

In the paper, a nonlinear control scheme of the UPQC has been applied to improve the operation of system under conditions of grid sags and nonlinear loads. First, the nonlinear system model in the dq synchronous reference frame is achieved. Then, for series active filters, the load voltages in dq components are designed, based on FL and resonant control for shunt active filters, grid current controllers in dq components are designed, depending on only FL. Simulation results for UPQC are given to verify the effectiveness of the proposed control scheme.

2. SYSTEM MODELING

The circuit configuration of the unified power quality conditioner is shown in Figure 1, in which a series active filter known as a compensator consists of a series transformer, LC filters, and voltage source inverter, and a shunt active filter referred to as a shunt compensator is composed of L filter and voltage source inverter. Both compensators are connected through a DC-link capacitor.

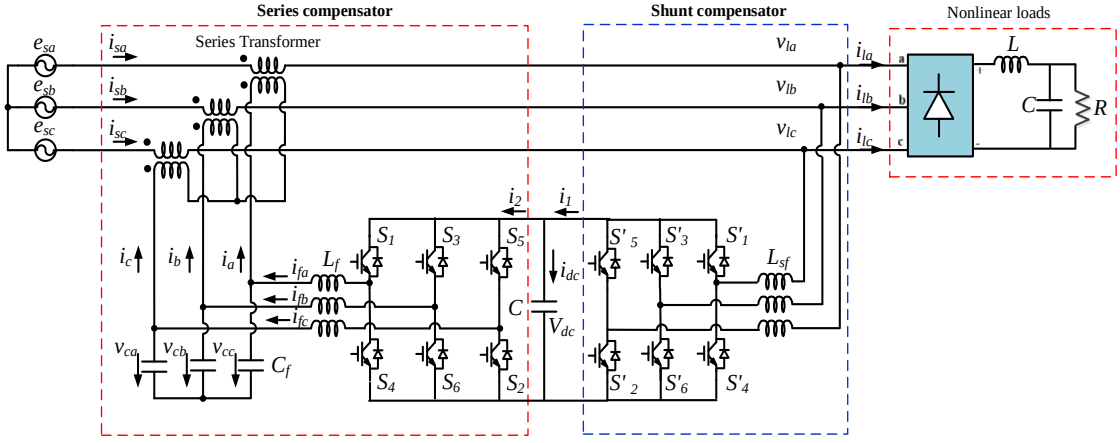

Figure 1. Circuit configuration of UPQC.

2.1. Series compensator

Modeling of series compensator system in synchronous dq reference frame can be expressed as [15, 16]

$$\dot{I}_{fdq} = \frac{1}{L_f} V_{dq} - \frac{1}{L_f} V_{cdq} - j\omega I_{fdq} \tag{1}$$

$$\dot{V}_{cdq} = \frac{1}{C_f} I_{dq} - \frac{1}{C_f} I_{fdq} - j\omega v V_{cdq} \tag{2}$$

where L_f is the filter inductance, C_f is the filter capacitance, V_{dq} is the dq axis inverter output voltages, V_{cdq} is the capacitor voltages in dq axis, I_{fdq} is the inverter output currents in dq axis, I_{dq} is the output currents of the series compensator in dq axis, and ω is the grid angle frequency.

From (1) to (2), a state-space modeling of the system is obtained as

$$\begin{bmatrix} \dot{I}_{fd} \\ \dot{I}_{fq} \\ \dot{V}_{cd} \\ \dot{V}_{cq} \end{bmatrix} = \begin{bmatrix} 0 & \omega & -1/L_f & 0 \\ -\omega & 0 & 0 & -1/L_f \\ 1/C_f & 0 & 0 & \omega \\ 0 & 1/C_f & -\omega & 0 \end{bmatrix} \begin{bmatrix} I_{fd} \\ I_{fq} \\ V_{cd} \\ V_{cq} \end{bmatrix} + \begin{bmatrix} 1/L_f & 0 \\ 0 & 1/L_f \\ 0 & 0 \\ 0 & 0 \end{bmatrix} \begin{bmatrix} V_d \\ V_q \end{bmatrix} + \begin{bmatrix} 0 \\ 0 \\ I_d/C_f \\ I_q/C_f \end{bmatrix} \quad (3)$$

2.2. Shunt compensator

Modelling of the shunt compensator system in a synchronous dq reference frame can be expressed as [17]

$$v_{ld} = R_{sf} i_{sfd} + L_{sf} \frac{di_{sfd}}{dt} - \omega L_{sf} i_{sfq} + v_{di} \quad (4)$$

$$v_{lq} = R_{sf} i_{sfq} + L_{sf} \frac{di_{sfq}}{dt} + \omega L_{sf} i_{sfd} + v_{qi} \quad (5)$$

where R_{sf} is the filter resistance, L_{sf} is the filter inductance, v_{dqi} is the dq axis inverter output voltages, v_{ldq} is the dq axis load voltages, i_{sfdq} is the dq axis output currents of shunt compensator, and ω is the grid angle frequency.

Balancing the input and output power of the shunt compensator can be expressed as

$$P_{in} = 1.5\left(v_{ld} i_{sfd} + v_{lq} i_{sfq}\right) = 1.5 v_{lq} i_{sfq} = V_{dc} i_{dc} \quad (6)$$

where $v_{ld} = 0$ và $v_{lq} = E_{\max}$

Equation (6) can be written as

$$1.5 v_{lq} i_{sfq} = V_{dc} C \frac{dV_{dc}}{dt} + i_2 \quad (7)$$

where $i_2 = i_1 - i_{dc}$.

From (4) to (7), a state-space modeling of the system is rewritten as

$$\begin{bmatrix} \dot{i}_{sfd} \\ \dot{i}_{sfq} \\ \dot{V}_{dc} \end{bmatrix} = \begin{bmatrix} \frac{v_{ld}}{L_{sf}} - \frac{R_{sf}}{L_{sf}} i_{sfd} - \omega i_{sfq} \\ \frac{v_{lq}}{L_{sf}} - \frac{R_{sf}}{L_{sf}} i_{sfq} + \omega i_{sfd} \\ \frac{3}{2CV_{dc}}\left(v_{lq} i_{sfq}\right) - \frac{1}{C} i_{dc} \end{bmatrix} + \begin{bmatrix} 0 \\ -\frac{1}{L_{sf}} \\ 0 \end{bmatrix} v_{qi} + \begin{bmatrix} -\frac{1}{L_{sf}} \\ 0 \\ 0 \end{bmatrix} v_{di} \quad (8)$$

3. CONTROL OF UPQC

In this section, the design of the proposed controllers depending on the FL control and resonant control is performed for series compensator and only FL control is applied for shunt compensator of UPQC so that the load voltages are controlled to reach rated values and kept almost sinusoidal and the grid currents are also maintained to be sinusoidal under grid voltage sags as well as nonlinear load conditions.

3.1. Load voltage compensation using a series compensator

The fundamental principle of the FL technique is that the nonlinear system is linearized by differentiating the system outputs until the variables of the input appear [15, 18].

The dynamic model of the series compensator in (3) using FL is expressed as

$$x=\begin{bmatrix} I_{fd} & I_{fq} & V_{cd} & V_{cq}\end{bmatrix}^T; u=\begin{bmatrix} V_d & V_q\end{bmatrix}^T; y=\begin{bmatrix} V_{cd} & V_{cq}\end{bmatrix}^T$$

To produce a clear relationship between the outputs $y_{i=1,2}$ and the inputs $u_{i=1,2}$, each output must be differentiated until a control input occurs.

$$\begin{bmatrix}\ddot{y}_1\\ \ddot{y}_2\end{bmatrix}=F(x)+G(x)\begin{bmatrix}u_1\\ u_2\end{bmatrix} \tag{9}$$

Then, the control law is given as

$$\begin{bmatrix}V_d^*\\ V_q^*\end{bmatrix}=\begin{bmatrix}u_1\\ u_2\end{bmatrix}=G^{-1}(x)\left[-F(x)+\begin{bmatrix}v_1\\ v_2\end{bmatrix}\right] \tag{10}$$

where

$$F(x)=\begin{bmatrix}\frac{2}{C_f}\omega I_{fq}-\left(\frac{1}{L_fC_f}+\omega^2\right)V_{cd}-\frac{1}{C_f}\dot{I}_d-\frac{1}{C_f}\omega I_q\\ -\frac{2}{C_f}\omega I_{fd}-\left(\frac{1}{L_fC_f}+\omega^2\right)V_{cq}-\frac{1}{C_f}\dot{I}_q+\frac{1}{C_f}\omega I_d\end{bmatrix};\quad G^{-1}(x)=\begin{bmatrix}L_fC_f & 0\\ 0 & L_fC_f\end{bmatrix}$$

and v_1 and v_2 are new control inputs.

A expected dynamic response is developed as follows

$$\begin{bmatrix}v_1\\ v_2\end{bmatrix}=\begin{bmatrix}\ddot{y}_1^*+k_{11}\dot{e}_1+k_{12}e_1+k_{13}\int e_1dt\\ \ddot{y}_2^*+k_{21}\dot{e}_2+k_{22}e_2+k_{23}\int e_2dt\end{bmatrix} \tag{11}$$

where $e_1=y_1^*-y_1$, and $e_2=y_2^*-y_2$. y_1^* and y_2^* are the desired values of the y_1 and y_2, respectively.

The error dynamics can be formulated in (11) as follows

$$\begin{aligned}&\ddot{e}_1+k_{11}\ddot{e}_1+k_{12}\dot{e}_1+k_{13}e_1=0\\ &\ddot{e}_2+k_{21}\ddot{e}_2+k_{22}\dot{e}_2+k_{23}e_2=0\end{aligned} \tag{12}$$

which are stable if the gains k_{11}, k_{12}, k_{13}, k_{21}, k_{22}, and k_{23} are positive [15].

Under the conditions of the grid voltage sag, the reference values of voltages for the series compensator consists of the components of DC voltage and second-order voltage harmonics. Thus, to obtain the tracking controllers, the proportional integral plus resonant regulators have been applied to remove the voltage errors in the steady-state. For tracking the references of the dq-axis components, the resonant frequency for regulators is chosen to be double fundamental frequency (2ω). So, the new control inputs can be expressed in the Laplace domain as follows

$$\begin{bmatrix} v_1 \\ v_2 \end{bmatrix} = \begin{bmatrix} s^2 y_1^* + k_{11} s e_1 + k_{12} e_1 + k_{13} \dfrac{e_1}{s} + \dfrac{k_r s}{s^2 + (2\omega)^2} e_1 \\ s^2 y_2^* + k_{21} s e_2 + k_{22} e_2 + k_{23} \dfrac{e_2}{s} + \dfrac{k_r s}{s^2 + (2\omega)^2} e_2 \end{bmatrix} \tag{13}$$

where k_r is a resonant gain.

To have an exact controller, the control inputs of (13) can be written as

$$\begin{bmatrix} u_1 \\ u_2 \end{bmatrix} = \begin{bmatrix} L_f C_f \left[v_1 - \dfrac{2}{C_f} \omega I_{fq} + \left(\dfrac{1}{L_f C_f} + \omega^2 \right) V_{cd} + \dfrac{1}{C_f} \dot{I}_d + \dfrac{1}{C_f} \omega I_q \right] \\ L_f C_f \left[v_2 + \dfrac{2}{C_f} \omega I_{fd} + \left(\dfrac{1}{L_f C_f} + \omega^2 \right) V_{cq} + \dfrac{1}{C_f} \dot{I}_q - \dfrac{1}{C_f} \omega I_d \right] \end{bmatrix} \tag{14}$$

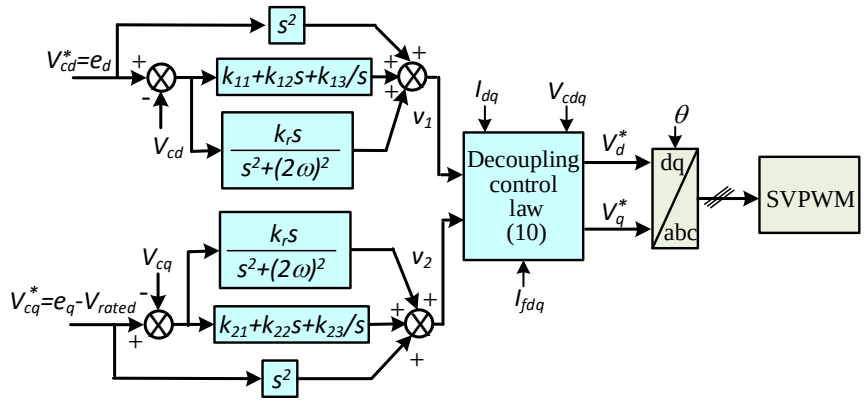

Figure 2. Block diagram of the proposed series compensator control scheme.

Figure 2 shows the block diagram of the proposed controller for the series compensator, in which the capacitor voltages in the dq-axis are regulated by using feedback linearization plus resonant controllers. The outputs of the controller (V_d^*, V_q^*) are transformed into phase voltage references (v_a^*, v_b^*, v_c^*), in which phase angle (θ) can be estimated using a second-order generalized integrator [19]. Then, these phase voltage references are used for space vector pulse-width modulation (SVPWM).

3.2. Grid current compensation using shunt compensator

The dynamic model of the shunt compensator in (8) using FL is expressed as

$$x = \begin{bmatrix} i_{sfd} & i_{sfq} & V_{dc} \end{bmatrix}^T ; u = \begin{bmatrix} v_{ld} & v_{lq} \end{bmatrix}^T ; y = \begin{bmatrix} i_{sfd} & V_{dc} \end{bmatrix}^T$$

Differentiating $y_1=i_{sfd}$ and $y_2=V_{dc}$ until a control input appears

$$\begin{bmatrix} \dot{y}_1 \\ \ddot{y}_2 \end{bmatrix} = A(x) + E(x)\begin{bmatrix} u_1 \\ u_2 \end{bmatrix} \tag{15}$$

The control law is obtained as

$$\begin{bmatrix} v_{ld}^* \\ v_{lq}^* \end{bmatrix} = \begin{bmatrix} u_1 \\ u_2 \end{bmatrix} = E^{-1}(x)\left[-A(x) + \begin{bmatrix} \gamma_1 \\ \gamma_2 \end{bmatrix}\right] \tag{16}$$

where

$$A(x) = \begin{bmatrix} \dfrac{v_{ld}}{L_{sf}} - \dfrac{R_{sf}}{L_{sf}} i_{sfd} - \omega i_{sfq} \\ \dfrac{3v_{lq}}{2CV_{dc}}\left(\dfrac{v_{lq}}{L_{sf}} - \dfrac{R_{sf}}{L_{sf}} i_{sfq} + \omega i_{sfd}\right) - \dfrac{3i_{sfq}v_{lq}}{2CV_{dc}^2}\left(\dfrac{3\left(i_{sfq}v_{lq}\right)}{2CV_{dc}} - \dfrac{i_2}{C}\right) - \dfrac{1}{C} i_2 \end{bmatrix};$$

$$E^{-1}(x) = \begin{bmatrix} L_f C_f & 0 \\ 0 & L_f C_f \end{bmatrix}$$

and v_1 and v_2 are new control inputs.

A desired dynamic response is developed as follows

$$\begin{bmatrix} \gamma_1 \\ \gamma_2 \end{bmatrix} = \begin{bmatrix} \dot{y}_1^* + k_{31}e_3 + k_{32}\int e_3 dt \\ \ddot{y}_2^* + k_{41}\dot{e}_4 + k_{42}e_4 + k_{43}\int e_4 dt \end{bmatrix} \tag{17}$$

Where $e_3 = y_1^* - y_1$, and $e_4 = y_2^* - y_2$. y_1^* and are the reference values of the y_1 and y_2, respectively.

The error dynamics can be formulated in (17) as

$$\begin{aligned} \dddot{e}_3 + k_{31}\ddot{e}_3 + k_{32}\dot{e}_3 + k_{32}e_3 = 0 \\ \dddot{e}_4 + k_{41}\ddot{e}_4 + k_{42}\dot{e}_4 + k_{43}e_4 = 0 \end{aligned} \tag{18}$$

which are stable if the gains k_{31}, k_{32}, k_{41}, k_{42} and k_{43} are positive [8].

To get the exact controller, the control inputs of (17) can be written as

$$\begin{bmatrix} u_1 \\ u_2 \end{bmatrix} = \begin{bmatrix} L_{sf}v_1 - \omega L_{sf} i_{fq} + R_{sf} i_{fd} \\ \dfrac{2CL_{sf}V_{dc}}{3E_{\max}} v_2 + \omega L_{sf} i_{fd} + R_{sf} i_{fq} + \dfrac{2L_{sf}V_{dc}}{3E_{\max}} i_2 + \dfrac{L_{sf}}{V_{dc}} i_{fq}\left\{\dfrac{3}{2V_{dc}} E_{\max} i_{fq} - \dfrac{i_2}{C}\right\} \end{bmatrix} \tag{19}$$

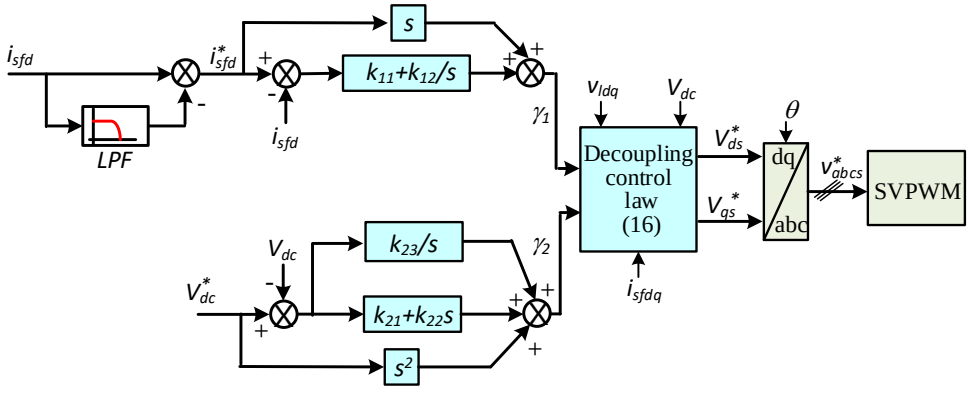

Figure 3. Block diagram of the proposed shunt compensator control scheme.

Figure 3 shows the block diagram of the proposed controller for the shunt compensator. To compensate current harmonics caused by nonlinear loads, the d-axis current is compared its reference obtained from low-pass filter (LPF) through applying feedback linearization control. Likewise, DC-link voltage based on FL is controlled to reach its rated value. The outputs of the controller ($v_{as}^*, v_{bs}^*, v_{cs}^*$) have been used to generate pulses by SVPWM [12].

4. SIMULATION RESULTS

The simulations using PSIM software have been done for the nonlinear loads in order to verify the effectiveness of the proposed method. The parameters of loads, series compensator, and shunt compensator are given in Tables 1, 2, and 3, respectively. The parameters of controllers for UPQC are given in the Tables 4 and 5.

Table 1. Parameters of nonlinear loads

Parameters	Values
Resistor	15 Ω
Inductor	1 mH
Capacitor	220 µF

Table 2. Parameters of the series compensator

Parameters	Values
Grid voltage	180 V_peak/ 60 Hz
DC link capacitor	340 µF
The inductor and capacitor of filters	0.01 mH, 10 µF
Switching frequency	10 kHz
Series transformers	3 kVA, 180/180 V

Table 3. Parameters of shunt compensator

Parameters	Values
Grid voltage	180 V_peak/ 60 Hz
DC-link voltage	340 V
Switching frequency	10 kHz
Filter inductor	2 mH
Filter resistor	0.05 Ω

Table 4. Parameters of controllers for series compensator

Type of controller		Controller gains
PI control	Current controller	$k_p = 16.2$ $k_i = 12100$
	Voltage controller	$k_{pv} = 0.34$ $k_{iv} = 871$
Proposed control		$k_{11} = k_{21} = 2.05 \times 10^3$ $k_{12} = k_{22} = 3.2 \times 10^6$ $k_{13} = k_{23} = 1.5 \times 10^9$ $k_r = 1200$

Table 5. Parameters of controllers for shunt compensator

Type of controller		Controller gains
PI control	Current controller	$k_{pi} = 0.6$ $k_{ii} = 15$
	Voltage controller	$k_{pvdc} = 0.072$ $k_{ivdc} = 0.448$
Proposed control		$k_{31} = 160$ $k_{32} = 12786.42$ $k_{41} = 660$ $k_{42} = 127856$ $k_{43} = 7455360$

The control performance of the UPQC with the PI control in the conditions of grid voltage sags and nonlinear loads is shown in Figure 4. As shown in Figure 4 (a), the grid voltage sags are assumed to be unbalanced, in which voltages of phases B and C also drop to 50% for 40 ms (from 1.48 to 1.52 seconds). The load currents, load voltages, and grid currents are illustrated in Figures 4 (b), (c), and (d), respectively. As can be clearly seen, the waveforms of the load voltages and grid currents are sinusoidal but still have some distortions.

In the same simulation conditions as the PI control method, the control performance of the UPQC using the proposed method is shown in Figure 5. Figure 5 (c) shows the load voltages, which are maintained at rated values regardless of the grid voltages drop, as illustrated in Figure 5 (a). The load currents and grid currents are illustrated in Figures 5 (b) and (d), respectively. With the proposed strategy, load voltages and grid currents are much better than those using PI ones, as seen in Figure 4.

Figures 6 and 7 show the Fast Fourier Transform (FFT) analysis for both PI and proposed controllers, respectively. It is seen that for the two methods, the waveforms of grid voltages are similar, which are imbalanced, and the load current is much distorted with the harmonics of 3rd, 5th, 7th order, and other higher order components. With only a linear PI regulator, it is illustrated from the results in Figure 9 (b) that, the series compensator of the UPQC cannot inject the components of the required voltages fully and the voltages of the series compensator can also contain the components of undesired 2nd harmonics, which affect the load voltages. By using the FL with the resonant controller for the series compensator, its control performance is considerably improved, but the load voltages still exist in the components of the higher-order harmonics as shown in Figure 6 (c). With the proposed method, it is obviously seen in Figure 7 (c) that the load voltages only contain the fundamental components.

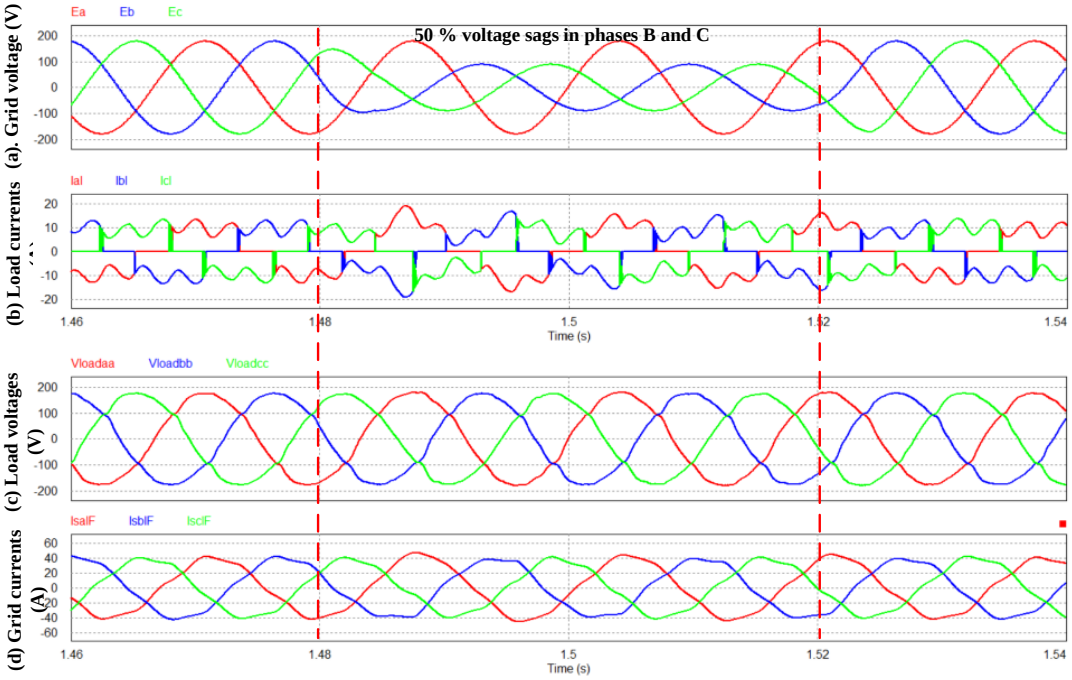

Figure 4. Dynamic responses of UPQC under the conditions of grid voltage sags and nonlinear loads using PI controller.

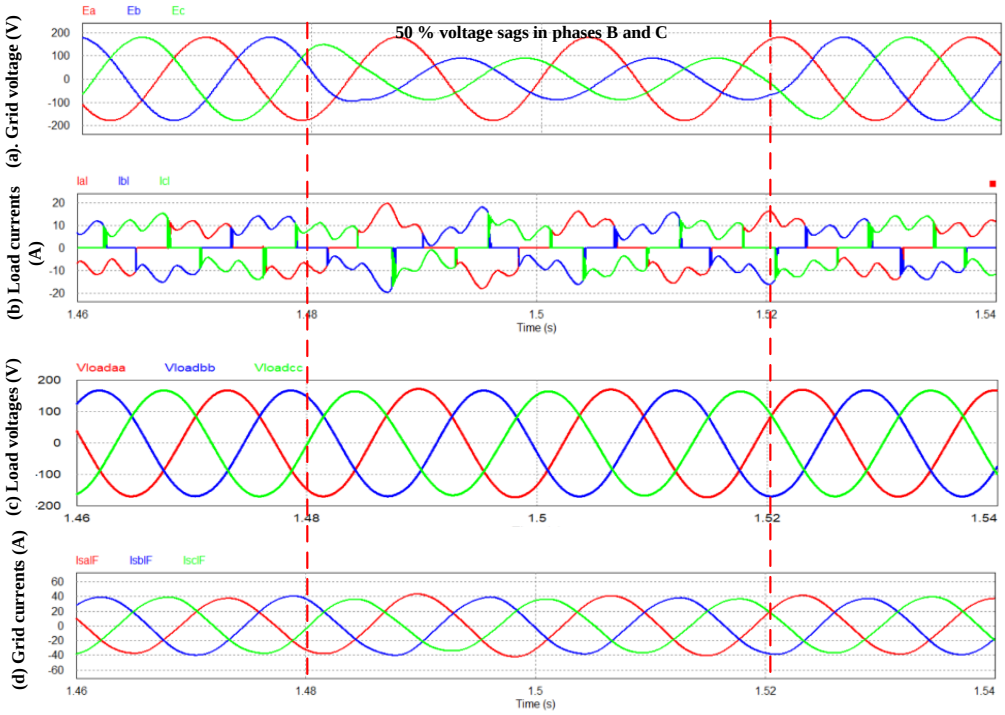

Figure 5. Dynamic responses of UPQC under the conditions of grid voltage sags and nonlinear loads using the proposed controller.

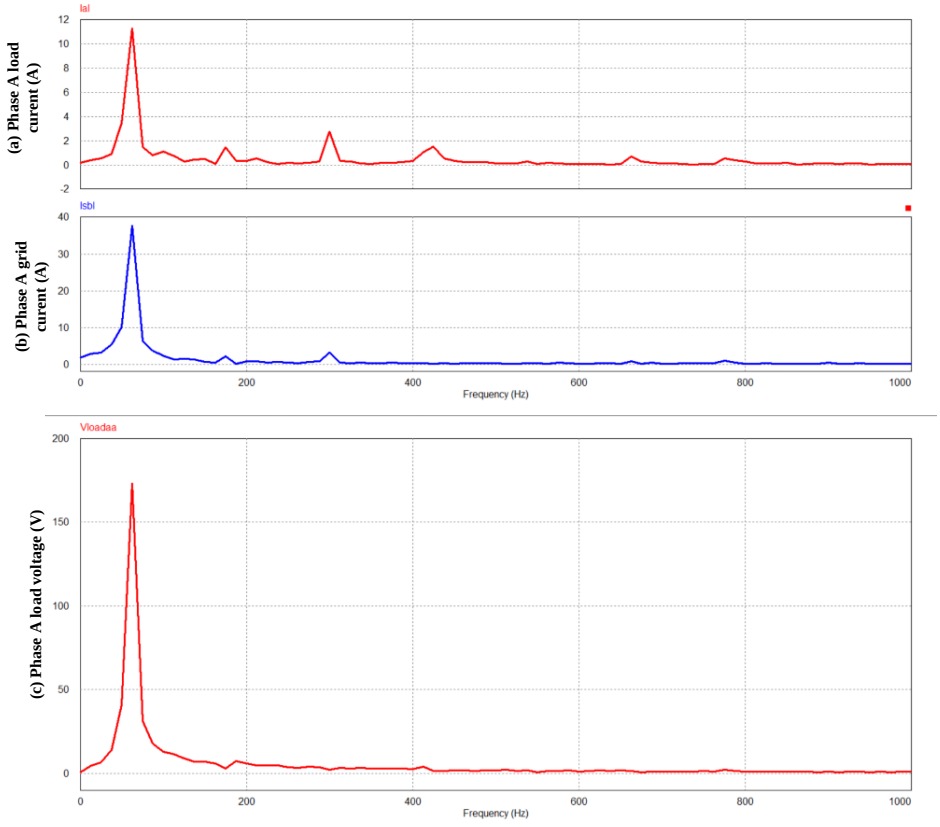

Figure 6. FFT spectra of the load current, grid current, and load voltage using the PI controllers

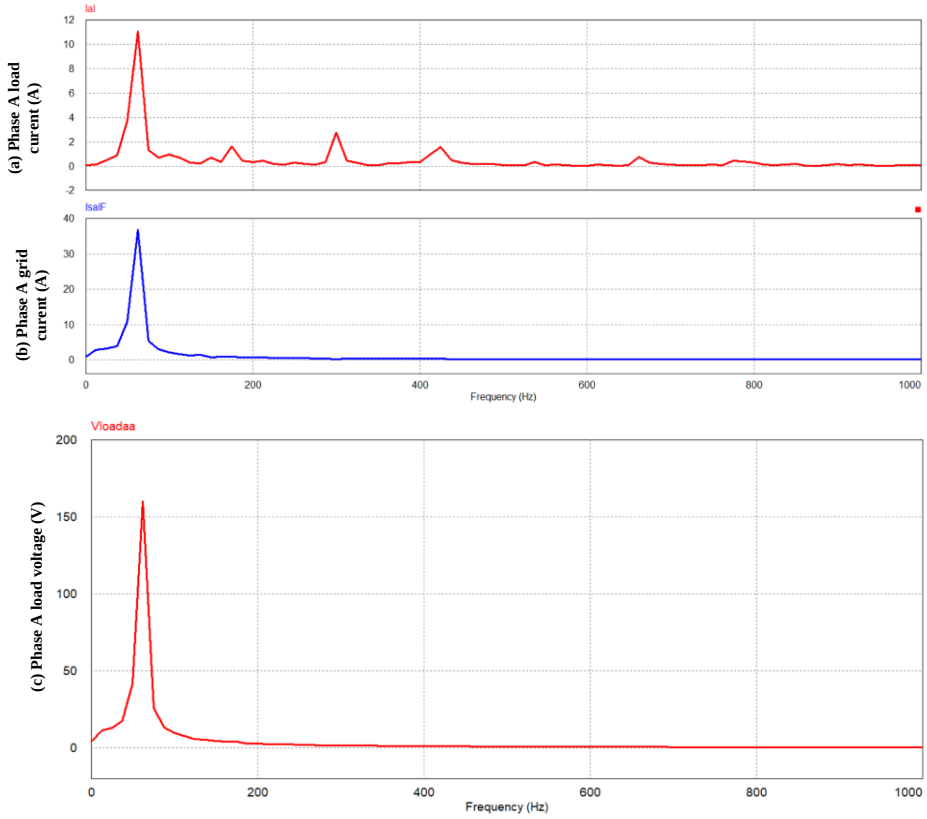

Figure 7. FFT spectra of the load current, grid current, and load voltage using the proposed controllers

Table 6. Comparison of THD of three-phase load voltages and grid currents using PI and proposed controllers

Type of controller	THD (%)					
	PI control			Proposed control		
	Phase A	Phase B	Phase C	Phase A	Phase B	Phase C
Load voltages	4.78	4.77	4.76	1.04	1.03	1.04
Grid currents	7.67	7.72	7.65	3.51	3.34	3.45

As seen in Table 6, the total harmonic distortion (THD) for load voltages and grid currents in the proposed controller gives better results with lower THD, compared with the conventional PI one.

5. CONCLUSION

The paper proposed the UPQC control scheme based on the nonlinear control technique with or without resonant control. The feasibility of the proposed control strategy was tested through simulation tests, where the load voltages are regulated to reach the rated value and both waveforms of load voltages and grid currents are controlled to become almost sinusoidal in the cases of grid voltage sags and nonlinear loads. The proposed control has shown better performance than the PI method. Also, with the proposed scheme, the UPQC can be extended to apply for both unbalanced and distorted grid voltages effectively in the upcoming research.

REFERENCES

1. Math H. Bollen - Understanding Power Quality Problems: Voltage Sags and Interruptions, Wiley-IEEE Press, 2000. https://ieeexplore.ieee.org/servlet/opac?bknumber=5270869
2. Math M. Bollen - Understanding power quality problems, voltage sags and interruptions, Wiley-IEEE Press, 2000. https://ieeexplore.ieee.org/servlet/opac?bknumber=5270869
3. Khalifa Al H., Thanh Hai N., Naji Al S. - An improved control strategy of 3P4W DVR systems under unbalanced and distorted voltage conditions, Electrical Power and Energy Systems **98** (2018) 233-242. https://doi.org/10.1016/j.ijepes.2017.12.001
4. Babaei E., Kangarlu M. F., and Sabahi M. - Mitigation of voltage disturbances using dynamic voltage restorer based on direct converters, IEEE Transactions on Power Electronics 25 (4) (2010) 2676-2683. https://10.1109/TPWRD.2010.2054116
5. Kim H. and Sul S.-K. - Compensation voltage control in dynamic voltage restorers by use of feed forward and state feedback scheme, IEEE Transactions on Power Electronics **20** (5) (2005) 1169-1177. https://10.1109/TPEL.2005.854052
6. Khadkikar V. and Chandra A. - UPQC-S: a novel concept of simultaneous voltage sag/swell and load reactive power compensations utilizing series inverter of UPQC, IEEE Transactions on Power Electronics **26** (9) (2011) 2414-2425. https://10.1109/TPEL.2011.2106222
7. Peng F. Z., -Application issues of active power filters, IEEE Industry Applicattions Magazine, **4** (1998) 21-30. https://10.1109/2943.715502
8. Tang Y., Loh P. C., Wang P., Choo F. H., Gao F., and Blaabjerg F. - Generalized design of high performance shunt active power filter with output LCL filter, IEEE Transactions on Industrial Electronics **59** (3) (2012) 1443-1452. https://10.1109/TIE.2011.2167117
9. Trinh Q. N. and Lee H. H., -An advanced current control strategy for three phase shunt active power filters, IEEE Transactions on Industrial Electronics **60** (12) (2013) 5400-5410. https://10.1109/TIE.2012.2229677
10. Tangtheerajaroonwong W., Hatada T., Wada K., and Akagi H.,-Design and performance of a transformerless shunt hybrid filter integrated into a threephase diode rectifier, IEEE Transactions on Power Electronics **22** (5) (2007 1882-1889. https:// 10.1109/TPEL.2007.904166
11. Patel H. and Agarwal V., -Control of a stand-aloneinverter-based distributed generation source for voltage regulation and harmonic compensation, IEEE Transactions Power Delivery **23** (2) (2008) 1113-1120. https://10.1109/TPWRD.2007.915890
12. Trinh Q.-N. and Lee H.-H. - Improvement of unified power quality conditioner performance with enhanced resonant control strategy, IET Generation Transmission Distribution **8** (12) (2014) 2114-2123. https://10.1049/iet-gtd.2013.0636
13. Trinh Q.N., Lee H.H. - An enhanced grid current compensator for grid-connected distributed generation under nonlinear loads and grid voltage distortions. IEEE Transactions on Industrial Electronics **61** (12) (2014) 6528–37. https:// 10.1109/TIE.2014.2320218
14. Kim D-E, Lee D-C. - Feedback linearization control of three-phase UPS inverter system. IEEE Transactions on Industrial Electronics **57** (3) (2010) 963-968. https:// 10.1109/TIE.2009.2038404
15. Van T.L., N. Nguyen M.D., L.T. Toi and T.T. Trang - Advanced control strategy of dynamic voltage restorers for distribution system using sliding mode control input-ouput

feedback linearization, Lecture Notes in Electrical Engineering **465** (2017) 521-531. https://doi.org/10.1007/978-3-319-69814-4_50

16. Van T.L., Nguyen T.H., Ho N.M., Doan X.N., and Nguyen T.H. - Voltage compensation scheme for DFIG wind turbine system to enhance low voltage ride-through capability, 10th International Conference on Power Electronics (ECCE Asia) (2019) 1334-1338. https://10.23919/ICPE2019-ECCEAsia42246.2019.8797269
17. Jang J.I., Lee D.C. - High performance control of three-phase PWM converters under nonideal source voltage, IEEE International Conference on Industrial Technology, (2006) 2791-27916. https://doi.org/10.1109/ICIT.2006.372693
18. Slotine J.-J. E. and Li W. - Applied nonlinear control, Englewood Cliffs, NJ: Prentice-Hall (1991) 207-271. https://books.google.com.vn/books/about/Applied_Nonlinear_Control.html?id=HddxQgAACAAJ&redir_esc=y
19. Rodriguez P., Luna A., Aguilar R.S.M., Otadui I.E., Teodorescu R., Blaabjerg F. - A stationary reference frame grid synchronization system for three-phase grid-connected power converters under adverse grid conditions, IEEE Transactions on Power Electronics **27** (1) (2012) 99-112. https://10.1109/TPEL.2011.2159242

TÓM TẮT

ĐIỀU KHIỂN BỘ ĐIỀU HÒA CHẤT LƯỢNG ĐIỆN NĂNG ĐỒNG NHẤT TRONG TRƯỜNG HỢP SỤT ÁP LƯỚI VÀ TẢI PHI TUYẾN

Nguyễn Thị Thanh Trúc, Văn Tấn Lượng*, Huỳnh Nhật Quang

Trường Đại học Công Thương Thành phố Hồ Chí Minh

*Email: *luongvt@huit.edu.vn*

Trong bài báo này, chiến lược điều khiển dựa trên kỹ thuật điều khiển phi tuyến cho bộ điều hòa chất lượng điện thống nhất (UPQC) hay còn gọi là bộ lọc tích cực nối tiếp và bộ lọc tích cực song song, được đề xuất để bù cả điện áp tải và dòng điện lưới độ trễ điện áp và tải phi tuyến. Mô hình phi tuyến của hệ thống bao gồm bộ lọc tích cực nối tiếp và bộ lọc tích cực song song trong hệ tọa độ quay dq được thực hiện. Bộ điều khiển điện áp tải dựa vào FL và điều khiển cộng hưởng và dòng điện lưới trong thành phần dq dựa vào FL được thiết kế, phụ thuộc vào bộ lọc tích cực nối tiếp và song song tương ứng. Với chiến lược đề xuất, điện áp tải được điều chỉnh để đạt giá trị định mức và cả hai dạng sóng của điện áp tải và dòng điện lưới đều được điều khiển để trở nên gần như hình sin, so với bộ điều khiển tích phân tỷ lệ (PI). Kết quả mô phỏng được đưa ra nhằm chứng minh tính hiệu quả của phương pháp đề xuất.

Từ khóa: Điều hòa chất lượng điện thống nhất (UPQC), tải phi tuyến, lý thuyết phi tuyến, sụt điện áp.